The optical damage resistance and absorption spectra of LiNbO$_3$:Hf crystals

The optical damage resistance and absorption spectra of LiNbO$_3$:Hf crystals

Shuqi Li[1], Shiguo Liu[1], Yongfa Kong[1,3], Dongling Deng[2], Guangyu Gao[2], Yanbo Li[2], Hongchen Gao[2], Ling Zhang[1], Ziheng Hang[1], Shaolin Chen[1] and Jingjun Xu[1]

[1] The MOE Key Laboratory of Advanced Techniques and Fabrication for Weak-Light Nonlinear Photonics Material, Nankai University, Tianjin 300457, People's Republic of China
[2] College of Physical Science, Nankai University, Tianjin 300071, People's Republic of China

E-mail: kongyf@nankai.edu.cn (Y Kong)

Abstract
Highly HfO$_2$ doped lithium niobate crystals have been grown. The experimental results indicate that LiNbO$_3$:Hf (up to 4 mol%) can withstand the same light intensity, of 5×10^5 W cm^{-2}, as LiNbO$_3$:Mg (6.5 mol%). And the OH$^-$ absorption bands of these LiNbO$_3$:Hf crystals shift to 3487 cm^{-1} from the 3484 cm^{-1} for congruent pure LiNbO$_3$. The difference spectra and fitting treatments show that the OH$^-$ absorption peak corresponding to $(\mathrm{Hf_{Nb}^{4+}})^-$–OH$^-$ is located at 3500 cm^{-1}.

(Some figures in this article are in colour only in the electronic version)

1. Introduction

Lithium niobate (LiNbO$_3$, LN) is one of the most important synthetic crystals, which has good electro-optic, acousto-optic, elasto-optic, piezoelectric and nonlinear properties. Laser induced optical damage or so-called photorefraction was firstly found in LiNbO$_3$ and LiTiO$_3$ crystals at Bell laboratory [1]. This effect can be utilized as holographic information storage and optical amplification; on the other hand, it hinders the usage of LiNbO$_3$ as frequency doublers, Q-switchers and optical waveguides. Therefore, the suppression of optical damage is one of the most important objectives for LiNbO$_3$ optical devices. Zhong *et al* reported that the optical damage resistance ability of LiNbO$_3$ could be improved by two orders of magnitude by doping with 4.6 mol% of MgO [2]. Besides Mg^{2+}, several other damage resistance impurities, such as divalent Zn^{2+} [3], trivalent Sc^{3+} [4] and In^{3+} [5], have also been found having the same resistance to optical damage.

---

[3] Author to whom any correspondence should be addressed.

Recently, Kokanyan *et al* [6] reported that the light induced birefringence changes of LiNbO$_3$ crystal doped with 4 mol% of HfO$_2$ were comparable to that of 6 mol% MgO doped crystals. This phenomenon indicates that hafnium is another new damage-resistant element. However, Hf is a tetravalent ion and its valence further approaches that of Nb (5+). Besides the photorefractive properties, many other physical properties of Hf doped LiNbO$_3$ crystals are still not clear. In this paper, the optical damage resistance, OH$^-$ and UV–visible absorption spectra of Hf doped LiNbO$_3$ crystals are investigated. On the basis of these experimental results, the lattice site location of HfO$_2$ in LiNbO$_3$ crystals is also discussed.

2. Experimental procedure

2.1. Crystal preparation

Hf doped LiNbO$_3$ crystals were grown from a congruent melt by the balance-controlled Czochralski method along the *c*-axis. The pulling and the rotation rate were 1.0 mm h^{-1} and 12 rpm respectively. The starting materials were Li$_2$CO$_3$, Nb$_2$O$_5$ and HfO$_2$ with the purity of 99.99%. The congruent composition was selected as [Li]/[Nb] = 48.38/51.62. The amounts of HfO$_2$ introduced into the melt were 2, 4 and 6 mol%, which we referred to as LN:Hf$_2$, LN:Hf$_4$ and LN:Hf$_6$, respectively. Two pieces of thin plates were cut from the top part and tail part of each of the as-grown crystals for x-ray fluorescence analysis. Then these crystals were cut into 1 and 3 mm plates along the *y*-faces and polished. For comparison, we have also included a congruent LiNbO$_3$ crystal doped with 6.5 mol% of MgO (hereafter labelled as LN:Mg$_{6.5}$).

2.2. Measurements

Two methods were employed to investigate the optical damage resistance ability of these crystals. One of them is called the direct observing transmission light spot distortion method. An argon laser was focused by means of a convex lens onto the 3 mm crystal wafer placed in the focal plane. When the laser intensity exceeded a certain value, the transmitted light beam spots would be smeared and elongated along the *c*-axis with decreased intensities in the central part. The other is holographic measurement. Two mutually coherent and extraordinary polarized argon laser ($\lambda = 514.5$ nm) beams with equal intensity 600 mW cm^{-2} intersected at $\theta = 11°$ in the crystal. The grating vector was aligned along the *c*-axis to utilize the largest electro-optic coefficient r_{33}. The saturation of the photorefractive index change Δn was calculated from the following equation [7]:

$$\eta_{\text{max}} = \sin^2(\pi \Delta n_{\text{sat}} d / \lambda \cos \theta_{\text{cry}}). \tag{1}$$

Here λ is the wavelength outside the crystal, d is the crystal thickness, Δn_{sat} is the refractive index change on saturation, η_{max} is the maximum diffraction efficiency and θ_{cry} is the intersection half-angle between the signal and reference beams in the crystal.

The distribution coefficient was investigated by x-ray fluorescence analysis. For this study, the weight ratios of Hf and Nb in the top and the tail plates of the crystals and the polycrystal material left in the crucible were determined. The samples were cracked and milled to fine powder (diameter less than 30 μm) and then shaped into plates. The OH$^-$ absorption spectra and UV–visible absorption spectra were measured using 1 mm plates with a MAGNA-560 FT-IR spectrophotometer and a BECKMAN DU-8B spectrophotometer, respectively, with the incident light transmitting along the *y*-axis at room temperature.

(a) (b) (c) (d)
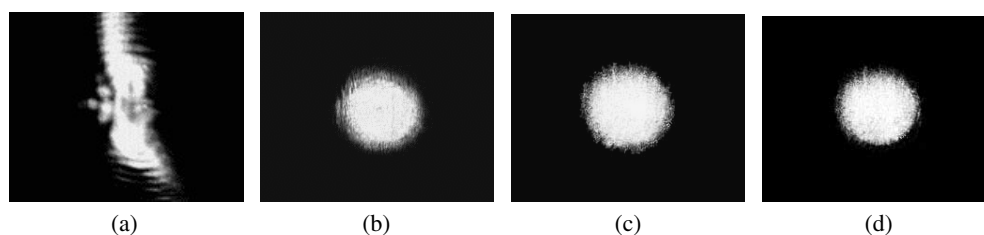
Figure 1. Distortion of the transmitted argon laser beam spot. (a) 2 mol% Hf; (b) 4 mol% Hf; (c) 6 mol% Hf; (d) 6.5 mol% Mg. The light intensity for (a) is 10^4 W cm^{-2} and 5×10^5 W cm^{-2} for (b), (c), and (d).

Table 1. The maximum change of refractive index (Δn_{sat}) of Hf doped and Mg doped lithium niobate crystals.

Sample No	Doping level	Δn (10^{-5})
LN:Hf$_2$	2.0 mol% Hf	2.2
LN:Hf$_4$	4.0 mol% Hf	0.87
LN:Hf$_6$	6.0 mol% Hf	0.84
LN:Mg$_{6.5}$	6.5 mol% Mg	0.78

3. Results and discussion

3.1. Optical damage resistance ability

The optical damage resistance ability was found to be about 700 W cm^{-2} for LN:Hf$_2$ crystal, which was one order of magnitude higher than that for the pure congruent one (about 20 W cm^{-2}) [2]. Figure 1 shows the distortion of the transmitted light spot when these wafers were irradiated with an Ar$^+$ ion laser. From this figure, we can see that LN:Hf$_4$ is able to withstand a laser power density of 5×10^5 W cm^{-2} without noticeable beam smearing, which is comparable to that observed for LN:Hf$_6$ and LN:Mg$_{6.5}$ crystals. However, for LN:Hf$_2$ under much lower power density, 10^4 W cm^{-2}, the transmitted light spot diffuses quickly along the *c*-axis, and at saturation the damage is so severe that no light spot in the central part is observable.

Table 1 shows the maximum change of refractive index (Δn_{sat}). The saturation index change of LN:Hf$_4$ is 8.7×10^{-6}, which is nearly equal to that of LN:Hf$_6$ and of LN:Mg$_{6.5}$, and approximately 2.5 times as low as that of LN:Hf$_2$. From table 1 and figure 1, we can see the optical damage of LiNbO$_3$ crystals is reduced by increasing the HfO$_2$ content. In fact, the optical damage resistance ability is improved in relation to the congruent pure crystal by four orders of magnitude as the doping concentration of HfO$_2$ reaches 4 mol% in the melt. It is known that the doping threshold of Mg in LiNbO$_3$ crystal is about 4.6 mol%. By comparing the optical damage resistance ability of Hf doped LiNbO$_3$ with that of LN:Mg$_{6.5}$, we consider that the concentration of Hf in LN:Hf$_4$ crystal has reached its doping threshold. This result is in good agreement with the former reports [6].

3.2. Distribution coefficient

The experiment result of x-ray fluorescence analysis shows that the distribution coefficient of Hf is 0.77, 0.93 and 0.84 for LN:Hf$_2$, LN:Hf$_4$ and LN:Hf$_6$, respectively. Generally, the distribution coefficient K_{eff} decreases with the increasing doping concentration [5], whereas these results are very different from what we expected.
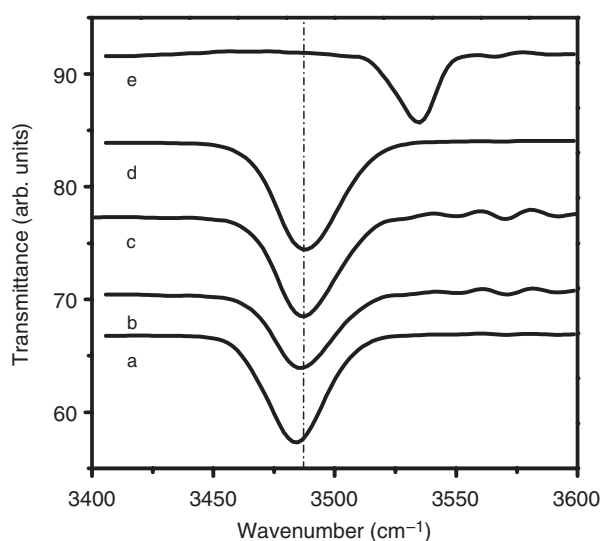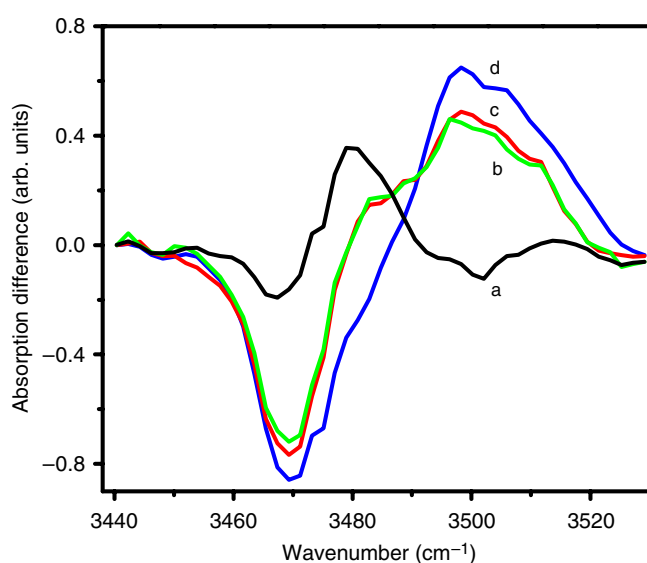
Figure 2. The OH$^-$ absorption spectra of LiNbO$_3$ crystals doped with Hf and Mg, respectively. (a) 2 mol% Hf; (b) 4 mol% Hf (the top part); (c) 4 mol% Hf (the bottom part); (d) 6 mol% Hf; (e) 6.5 mol% Mg. The absorption bands are located 3484, 3485, 3487, 3487 and 3535 cm^{-1} for (a), (b), (c), (d) and (e), respectively.

The distribution coefficient K_{eff} of Mg is about 1.2 near the doping threshold and slightly decreases for higher MgO doping concentrations. Therefore, the composition distribution of Mg makes it very difficult to grow MgO doped LiNbO$_3$ crystals with high composition homogeneity and optical quality. The K_{eff} of Hf for LN:Hf$_4$ is 0.93, which is nearer to 1 than that of Mg, so high quality LN:Hf$_4$ crystal may be easier to grow than the usually used LiNbO$_3$ crystal doped with 5 mol% MgO. Moreover, the K_{eff} varies in the range from 2 to 6 mol% and has a maximum near 4 mol% HfO$_2$, which means that K_{eff} may have a value quite close to 1 when the concentration of HfO$_2$ is about 4 mol%.

3.3. OH$^-$ absorption spectra

Figure 2 shows the OH$^-$ absorption spectra of LiNbO$_3$:Mg and LiNbO$_3$:Hf crystals. The absorption bands are located near 3484, 3487 and 3535 cm^{-1} for LiNbO$_3$ crystals doped with 2 and 6 mol% HfO$_2$ and 6.5 mol% MgO, respectively. The absorption band shifts from 3485 to 3487 cm^{-1} as the transmitted light changes from the top part to the bottom part of LN:Hf$_4$. It is known that the OH$^-$ absorption bands of doped LiNbO$_3$ crystals have obvious shifts from about 3484 cm^{-1} for pure LiNbO$_3$ to higher wavenumbers when the doping concentrations exceed thresholds. However, the shifts of Hf doped LiNbO$_3$ crystals are too weak to distinguish; consequently a difference method [8] was employed in this study.

In order to show the changes of absorption, the congruent pure crystal was measured, and differences between the spectra of doped and pure crystals were taken. Firstly, we translated the measured OH$^-$ transmittance spectra into absorption spectra. Secondly, we integrated these absorption spectra among a selected range of wavenumbers (from 3440 to 3530 cm^{-1}) and obtained the integration area. Then these absorption spectra were divided by their integration area; this process was defined as normalization. Finally, the normalized absorption spectra of doped crystals had subtracted from them the normalized absorption spectra of congruent pure LiNbO$_3$, giving the difference spectra for the doped crystals.
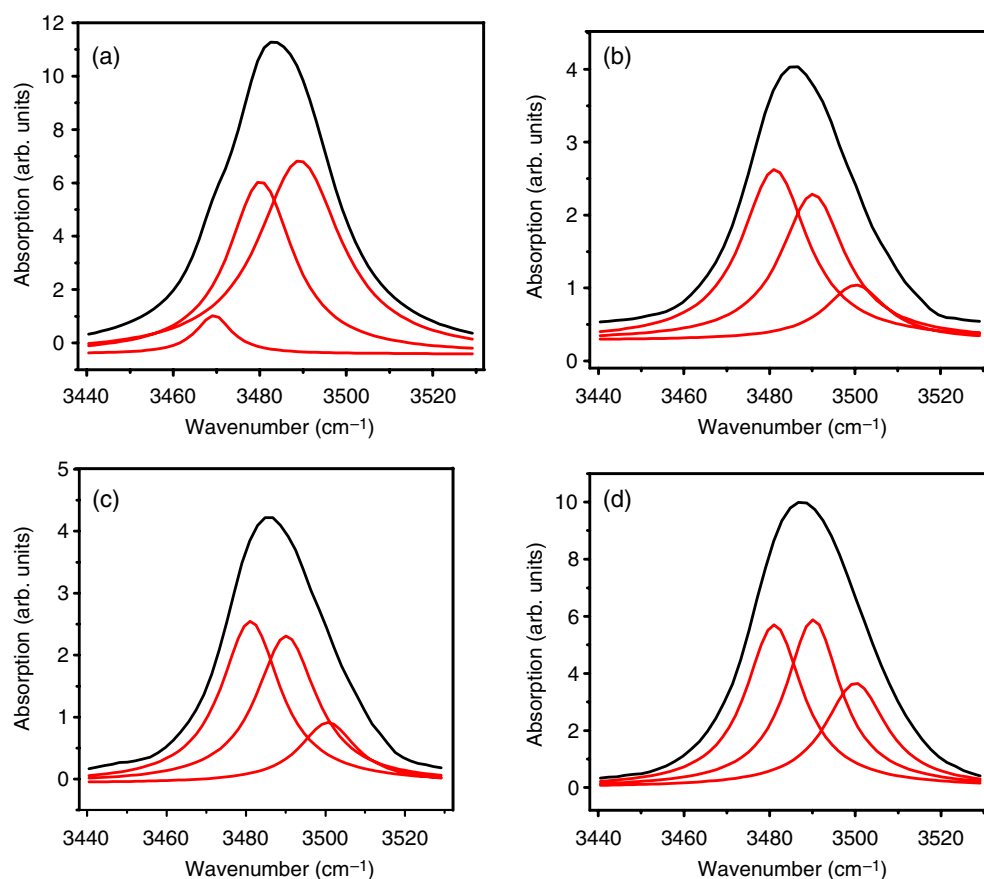
Figure 3. The OH$^-$ difference spectra of Hf doped LiNbO$_3$ crystals. (a) 2 mol% Hf; (b) 4 mol% Hf (the top part); (c) 4 mol% Hf (the bottom part); (d) 6 mol% Hf.

Table 2. The positions of component peaks in the OH$^-$ absorption spectra of Hf doped lithium niobate crystals.

Sample	Position of peaks (cm^{-1})		
LN:Hf$_2$	3469.0	3480.2	3489.2
LN:Hf$_4$ (the top part)	3481.2	3490.2	3500.2
LN:Hf$_4$ (the bottom part)	3481.1	3490.1	3500.6
LN:Hf$_6$	3481.1	3490.2	3500.1

Figure 3 shows the OH$^-$ difference spectra of LiNbO$_3$:Hf crystals. From this figure, we can see there is a big difference between the spectrum of LN:Hf$_2$ and those of the others: the former comprises three peaks, a stronger positive one in the middle part and a weaker negative one on each side; the latter consist of two peaks, a larger negative one in the lower wavenumber and a broader positive one at higher wavenumber. The two difference spectra of LN:Hf$_4$, from top to bottom have almost the same shape, which is similar to that for LN:Hf$_6$. As we know, 6 mol% Hf doping in LiNbO$_3$ has exceeded its threshold [6]; thus we can conclude that Hf ions have occupied normal Nb sites in LN:Hf$_4$ and LN:Hf$_6$ crystals.

According to the shape of the Hf doped LiNbO$_3$ difference spectra, the three decomposed peaks of the absorption band can be imagined. In order to find the peak caused by the influence of (Hf$_{Nb}^{4+}$)$^-$ (Hf located at normal Nb sites), these absorption spectra were respectively decomposed to three Lorentzian peaks by fitting. The fitting results are collected in table 2, and all results are also drawn in figure 4. For LN:Hf$_2$ crystal, three peaks are located at 3469, 3480 and 3489 cm^{-1}, which correspond to those of pure LiNbO$_3$ crystal [9], while for LN:Hf$_4$ and LN:Hf$_6$ crystals, the 3469 cm^{-1} absorption peak vanishes and a new 3500 cm^{-1} one arises. It is easily seen that the 3500 cm^{-1} peak intensity increases when the Hf doping concentration varies from 4 to 6 mol%. Therefore, this new absorption peak corresponds to the OH$^-$ stretching vibration in the (Hf$_{Nb}^{4+}$)$^-$–OH$^-$ defect complex, and this result further proves that 4 mol% of HfO$_2$ in the LiNbO$_3$ melt has reached its doping threshold.

Figure 4. The components of OH$^-$ absorption spectra of Hf doped LiNbO$_3$ crystals. (a) 2 mol% Hf; (b) 4 mol% Hf (the top part); (c) 4 mol% Hf (the bottom part); (d) 6 mol% Hf.

3.4. UV–visible absorption spectra

Figure 5 shows the UV–visible absorption spectra of the crystals. The absorption edge is defined as the corresponding wavelength where the absorption coefficient is equal to 20 cm^{-1}. The dashed line and the solid line represent the absorption spectra of LiNbO$_3$:Mg and LiNbO$_3$:Hf, respectively. For LiNbO$_3$ doped with 2, 4 and 6 mol% of HfO$_2$, the absorption edges are at 316.6, 315.9 and 316.1 nm, respectively (see the inset of figure 5). For 6.5 mol% MgO doped crystal, there is a shift to 310 nm.

The absorption edge is situated at 320 nm for the congruent sample and 303 nm for the stoichiometric sample [10]. In Mg doped LiNbO$_3$ crystals the UV edge shifts to shorter wavelength as the doping concentration goes below the threshold, and returns when it goes above the threshold [11]. Similar behaviour is observed for Hf doped LiNbO$_3$ crystals. However, the maximum blue shift of LiNbO$_3$:Hf is much lower than that of LiNbO$_3$:Mg. This difference may arise from their different valence states. If tetravalent hafnium ions are incorporated into Li sites, the crystal approaches the congruent one and the edge is close to 320 nm; while if divalent magnesium ions occupy Li sites, the crystal approaches the stoichiometric one and the edge is close to 303 nm.
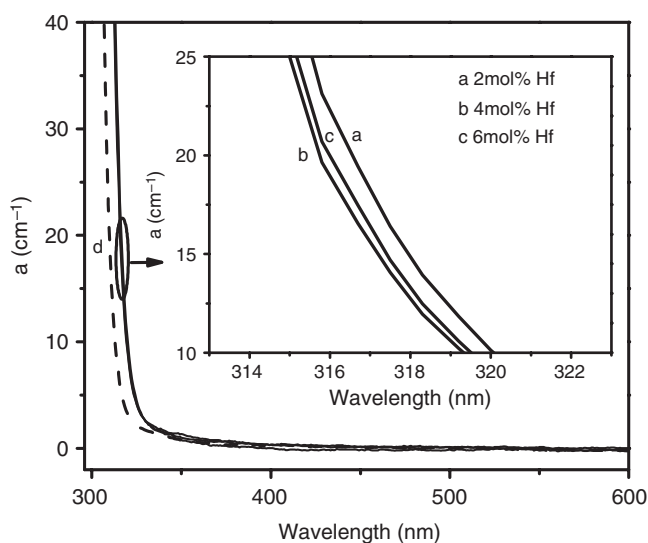
Figure 5. The UV–visible absorption spectra of the crystals. (a) 2 mol% Hf; (b) 4 mol% Hf; (c) 6 mol% Hf; (d) 6.5 mol% Mg.

3.5. Lattice site location mechanism

According to Li vacancy model [12], the excess Nb_2O_5 in congruent $LiNbO_3$ will exist as

$$3Nb_2O_5 = 5(Nb_{Li}^{4+})_{1/5}(V_{Li}^-)_{4/5}NbO_3. \qquad (2)$$
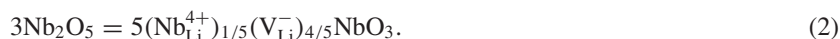
In this work, the content of excess Nb_2O_5 is 3.24 mol%, so 1.08 mol% Nb atoms occupy Li sites, forming antisite niobium ions (Nb_{Li}^{4+}), and charge neutrality is maintained by 4.32 mol% Li site vacancies (V_{Li}^-). When the doping content of HfO_2 is low, firstly antisite Nb^{5+} ions will be pushed away from Li sites to normal Nb sites in the following process:

$$3HfO_2 + 10(Nb_{Li}^{4+})_{1/5}(V_{Li}^-)_{4/5}NbO_3 = 12(Hf_{Li}^{3+})_{1/4}(V_{Li}^-)_{3/4}NbO_3 \qquad (3)$$
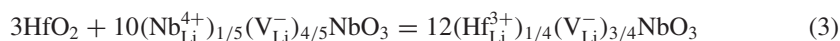
that proceeds until all antisite Nb^{5+} ions are exhausted. For this purpose only 1.62 mol% Hf is needed. However, our experimental results indicate that the doping threshold of Hf is about 4 mol% in the melt, so we consider, when the doping concentration is above 1.62 mol%, that a large number of Nb_{Li}^{4+} have disappeared and a portion of Hf ions may substitute for normal Li ions before they enter Nb sites in the following defect chemical equation:

$$HfO_2 + 4LiNbO_3 = 4(Hf_{Li}^{3+})_{1/4}(V_{Li}^-)_{3/4}NbO_3 + 2Li_2O. \qquad (4)$$
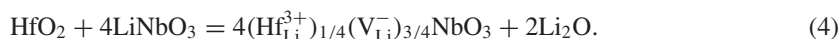
That process will not cease until the doping concentration of HfO_2 is about 4 mol% in the melt. The remaining Hf ions are likely to be then split between normal Li sites and Nb sites, in a ratio of 1:3 to maintain charge balance, with the defect chemical equation given by

$$3LiNbO_3 + 4HfO_2 = 3(Hf_{Li})_{1/3}Li_{2/3}Hf_{Nb}O_3 + 1/2\ Li_2O + 3/2\ Nb_2O_5. \qquad (5)$$

4. Conclusions

A series of Hf doped congruent lithium niobate crystals ranging from 2 to 6 mol% are presented. The threshold concentration of HfO_2 is found to be about 4 mol% in the melt. The optical damage resistance ability of $LiNbO_3$:Hf (4 mol%) crystal is four orders of magnitude higher

than that of the congruent pure one, the OH^- absorption band shifts to about 3487 cm^{-1} from the 3484 cm^{-1} for the congruent pure LiNbO$_3$ and the UV edge has a maximal blue shift. The difference spectra and fitting treatments show that the OH^- absorption peak related to the $(Hf_{Nb}^{4+})^- - OH^-$ defect complex is situated at 3500 cm^{-1}.

Acknowledgments

References

[1] Askin A, Boyd G D, Dziedzic J M, Smith R G, Ballman A A, Levinstein J J and Nassau K 1966 *Appl. Phys. Lett.* **9** 72
[2] Zhong G, Jin J and Wu Z 1980 *11th Int. Quantum Electronics Conf. (New York)* IEEE Cat. No. 80 CH 1561-0 p 631
[3] Volk T R, Rubinina N M, Pryalkin V I, Krasnikov V V and Volkov V V 1990 *Ferroelectrics* **109** 345
[4] Yamamoto J K, Kitamura K, Iyi N, Kimura S, Furukawa Y and Sato M 1992 *Appl. Phys. Lett.* **61** 2156
[5] Kong Y, Wen J and Wang H 1995 *Appl. Phys. Lett.* **66** 280
[6] Kokanyan E P, Razzari L, Cristiani I, Degiorgio V and Gruber J B 2004 *Appl. Phys. Lett.* **84** 1880
[7] Kogelnik H 1969 *Bell Syst. Tech. J.* **48** 2909
[8] Kong Y, Zhang W, Xu J, Yan W, Liu H, Xie X, Li X, Shi L and Zhang G 2004 *Infrared Phys. Technol.* **45** 281
[9] Kong Y, Zhang W, Chen X, Xu J and Zhang G 1999 *J. Phys.: Condens. Matter* **11** 2139
[10] Polgár K, Petér Á, Kovács L, Corradi G and Szaller Zs 1997 *J. Cryst. Growth* **177** 211
[11] Polgár K, Kovács L, Földvári I and Cravero I 1986 *Solid State Commun.* **59** 375
[12] Lerner P, Legras C and Dumas J P 1968 *J. Cryst. Growth* **3/4** 231